New Journal of Physics
The open access journal at the forefront of physics

Deutsche Physikalische Gesellschaft DPG
IOP Institute of Physics
Published in partnership with: Deutsche Physikalische Gesellschaft and the Institute of Physics

OPEN ACCESS

RECEIVED
18 January 2018

REVISED
23 April 2018

ACCEPTED FOR PUBLICATION
15 May 2018

PUBLISHED
31 May 2018

PAPER

Resonant interaction of slow light solitons and dispersive waves in nonlinear chiral photonic waveguide

A V Yulin[1], I V Iorsh[1] and I A Shelykh[1,2]

[1] ITMO University, Saint Petersburg, 197101, Russia
[2] Science Institute, University of Iceland, Dunhagi 3, IS-107, Reykjavik, Iceland

E-mail: i.iorsh@metalab.ifmo.ru

Keywords: chiral photonics, soliton, spin-momentum locking

Abstract

We study the structure of the elementary excitations and their propagation in chiral hybrid structure, comprising an array of two-level systems (TLSs) coupled to a one-dimensional photonic waveguide. The chirality is achieved via spin-locking effect, which in an ideal case gives perfect unidirectional excitation transport. We show that the application of transverse magnetic field which mixes the corresponding levels in TLS results in the emergence of the slow light mode in the photonic spectrum. Finally, we demonstrate the protocols of writing the signal to the slow light mode as well as reading it out with ultrashort optical pulses, which opens new avenues for the realization of optical memory devices based on chiral optical systems.

1. Introduction

Physics of systems with chirality is one of the current trends in modern science. In condensed matter the paragon example of the chiral system is represented by one-dimensional edge states forming in the regime of the quantum Hall effect [1] where chirality appears due to the breaking of the time inversion symmetry provided by the application of the external magnetic field. Besides, non-trivial topology of the bulk electronic structure related to the presence of strong spin–orbit interaction [2] can also result in the formation of gapless edge modes, which make the surface or interface of the material conducting, while leaving the interior insulating. This happens in the class of materials known as topological insulators [3]. In the domain of photonics, chiral edge states appear in photonic crystals with engineered Berry curvature of the photonic bands, photonic analogs of Hall effect [4–6] and topological insulators [7–10]. Effects of non-trivial topology were reported in the wide frequency range, from radio to optical frequencies [11].

Hybrid light–matter coupled systems can present certain advantages with respect to purely photonic or purely material ones. Indeed, in the regime of strong coupling these systems can support hybrid excitations known as polaritons. The typical example of the geometry where polaritons emerge is planar microcavity consisting of a pair of dielectric Bragg mirrors and one or several quantum wells with excitonic transition in resonance with cavity mode [12]. The presence of the photonic component in cavity polaritons make them robust against decoherence, while the material component is responsible for efficient polariton–polariton interactions leading to the pronounced nonlinear response [13]. Besides, it is possible to tune the system by application of external electric and magnetic fields [14]. This opens the possibility to engineer analogs of topological insulators based on polariton superlattices, where band inversion is achieved due to the interplay of the Zeeman splitting of the excitons induced by external magnetic field and TE–TM splitting of the confined photons [15–17].

On the other hand, there exists another simple and prospective way to organize chiral light–matter coupling based on employment of transverse spin angular momentum of light (SAM), which has recently attracted significant research interest [18, 19]. For 2d evanescent electromagnetic modes, e.g. surface plasmon polaritons, non-zero optical SAM density emerges due to the $\pi/2$ phase shift between the electric field projections onto the interface plane and to its normal [20]. Transverse character of electromagnetic waves leads to the spin-momentum

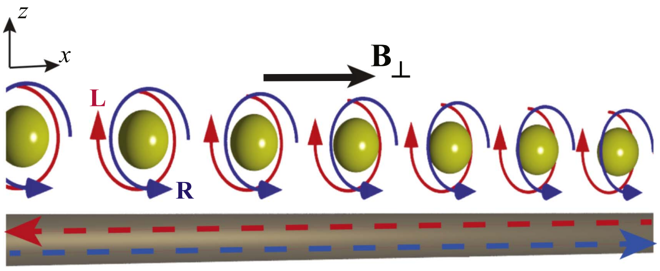

Figure 1. Schematic image of a TLS array over a chiral photonic waveguide.

locking: SAM projection is defined by the propagation direction of light [21, 22]. This effect represents optical analog of spin–orbit coupling and can be used in a variety of applications related to nanooptomechanics [23–25], topological photonics [26], electromagnetic routing [27], electromagnetically assisted unidirectional spin transfer [28].

It was recently suggested that SAM of confined electromagnetic modes propagating in quasi 1D fibers can be used for the engineering of quantum information networks of next generation [29, 30]. The proposed geometry consisted from regular one-dimensional array of two-level systems (TLSs), atoms or quantum dots placed on the surface of the fiber and resonantly coupled to the evanescent mode propagating in it (see figure 1(a)). The current state of technology allows fabrication of these kind of systems [31] and monitoring of their physical properties such as Bragg reflection spectrum [32, 33]. Transport of the collective excitations in these kind of systems will in focus of the present paper. We will consider both coupling of the fiber mode to regular array of discrete emitters and to a continuous 1D media which can be represented by e.g. semiconductor quantum wire or organic polymer chain placed on the surface of the photonic fiber (see figure 1(b)).

2. The model

We start from the Hamiltonian $\hat{H}$ for the TLS array coupled to the photonic bath:

$$\hat{H} = \hat{H}_{\mathrm{phot}} + \hat{H}_{\mathrm{TLS}} + \hat{H}_c, \tag{1}$$

where the first term corresponds to the Hamiltonian of the chiral photonic reservoir:

$$\hat{H}_{\mathrm{phot}} = -\mathrm{i}\hbar v \int \mathrm{d}x [\hat{\varphi}^{(R)\dagger}(x)\partial_x\hat{\varphi}^{(R)}(x) - \hat{\varphi}^{(L)\dagger}(x)\partial_x\hat{\varphi}^{(L)}(x)], \tag{2}$$

where $\hat{\varphi}$ is the annihilation operator of the photonic mode, (R, L) define the mode polarization, and v is the mode velocity. Such type of the Hamiltonian can be realized in a number of systems: for example, it can be an edge of a photonic topological insulator [34]. Alternatively, this could be any guided mode in a one-dimensional waveguide—in this case the polarization index defines the direction of the optical SAM [35]. The mode velocity v is fixed and set to $2c/3$, where c is the speed of light in vacuum, which is a typical value for this kind of systems.

The Hamiltonian of the TLS array $\hat{H}_{\mathrm{TLS}}$ is given by

$$\hat{H}_{\mathrm{TLS}} = \sum_{j,\sigma=(R,L)} \Omega_{\perp} \sum_j [\hat{S}^{(R)}_{+,j}\hat{S}^{(L)}_{-,j} + \hat{S}^{(L)}_{+,j}\hat{S}^{(R)}_{-,j}], \tag{3}$$

where summation is taken over the TLSs position j, $\hat{S}$ are the spin operators satisfying the standard commutation relations, and $\Omega_{\perp}$ is proportional to the effective transverse magnetic field which mixes two polarizations. In the calculations, ϵ is set to 1 eV, and $\Omega_{\perp}$ is varying from 0 to 1 meV. The coupling Hamiltonian $\hat{H}_c$ is given by

$$\hat{H}_c = \Omega_R \sum_j \left[\hat{S}^{(R)}_{x,j} \int \mathrm{d}x\hat{\varphi}^{(R)}(x)\psi_j^*(x) + \hat{S}^{(L)}_{x,j} \int \mathrm{d}x\hat{\varphi}^{(L)}(x)\psi_j^*(x) + \mathrm{h.c.}\right], \tag{4}$$

where Ω_R is the characteristic coupling strength which is set to 0.5 meV, and $\psi_j(x)$ is the two-level system wavefunction which can be approximated by $\psi_j(x) = (2\pi L)^{-1/2}\mathrm{e}^{-(x-x_j)^2/2L^2}$, where L is the effective TLS dimension (set to 10 nm in the calculation). We then move to the mean field approximation and further treat $\varphi^{(R,\ L)}$ and $\hat{S}$ as complex-valued functions. It should be noted, that in the case when $\epsilon \gg \Omega_{\perp}, \Omega_R$ the rotating wave approximation may be used. Within this approximation, we neglect the amplitude φ_L (if it was initially absent) and obtain equations of motions using the Heisenberg equation. In the dimensionless units $t = (\Omega_R/\hbar)t, x = x/(v\hbar/\Omega_R)$ the equations read

$$\mathrm{i}\frac{\partial\varphi^{(R)}}{\partial t}+\mathrm{i}\frac{\partial\varphi^{(R)}}{\partial x}=\sum_j S_{-,j}^{(R)}(t)\psi_j(x), \tag{5}$$

$$\mathrm{i}\frac{\partial S_{-,j}^{(R)}}{\partial t}=-S_{z,j}^{(R)}\int \mathrm{d}x\varphi^{(R)}(x)\psi_j(x)-\Omega S_{z,j}^{(R)}S_{-,j}^{(L)}, \tag{6}$$

$$\frac{\partial S_{z,j}^{(R)}}{\partial t}=-\mathrm{Im}\left(S_{-,j}^{(R)}\int \mathrm{d}x\varphi^{(R)*}(x)\psi_j(x)\right)-\Omega\,\mathrm{Im}\,S_{-,j}^{(R)}S_{-,j}^{(L)*}, \tag{7}$$

$$\mathrm{i}\frac{\partial S_{-,j}^{(L)}}{\partial t}=-\Omega S_{z,j}^{(L)}S_{-,j}^{(R)}, \tag{8}$$

$$\frac{\partial S_{z,j}^{(L)}}{\partial t}=-\Omega\,\mathrm{Im}\,S_{-,j}^{(L)}S_{-,j}^{(R)*}, \tag{9}$$

where Ω are normalized to Ω_R. The equation of motion for $\hat{S}_{+,j}$ is omitted since these quantities can be directly obtained from the relation $S_{-,j}S_{+,j}+S_{z,j}^2=1/4$.

It is also instructive to move to the continuous limit by changing S_j to $S(x)$ and $\sum_j S_{-,j}\psi_j(x)$ to $\rho\int \mathrm{d}xS_-(x)\psi(x-x')$ where ρ is the TLS concentration. We also apply the approximation of an infinitely narrow kernel $\psi(x-x')=\sqrt{L}\,\delta(x-x')$. Then the equations (5)–(9) transform into

$$\mathrm{i}\frac{\partial\varphi^{(R)}}{\partial t}+\mathrm{i}\frac{\partial\varphi^{(R)}}{\partial x}=\rho S_-^{(R)}(t), \tag{10}$$

$$\mathrm{i}\frac{\partial S_-^{(R)}}{\partial t}=-S_z^{(R)}\varphi^{(R)}(x)-\Omega S_z^{(R)}S_-^{(L)}, \tag{11}$$

$$\frac{\partial S_z^{(R)}}{\partial t}=-\mathrm{Im}\,(S_-^{(R)}\varphi^{(R)*})-\Omega\,\mathrm{Im}\,S_-^{(R)}S_{-,j}^{(L)*}, \tag{12}$$

$$\mathrm{i}\frac{\partial S_-^{(L)}}{\partial t}=-\Omega S_z^{(L)}S_-^{(R)}, \tag{13}$$

$$\frac{\partial S_z^{(L)}}{\partial t}=-\Omega\,\mathrm{Im}\,S_-^{(L)}S_-^{(R)*}. \tag{14}$$

It is important to note that for zero magnetic field $\Omega=0$ the equations coincide with Maxwell–Bloch equations describing propagation of optical pulses in two-level media where there are well known self induced transparency (SIT) soliton, [36–38]. Indeed, in this case the problem can be formulated in terms of amplitudes of wavefunctions corresponding to the upper v_1 and the lower v_2 levels such that

$$S_-^{(R)}=\mathrm{i}v_1v_2^*\exp(2\mathrm{i}\xi\tau)$$

$$S_z^{(R)}=\frac{1}{2}(|v_1|^2-|v_2|^2).$$

The equations for the amplitudes of the wavefunctions and the photonic field have the form

$$\partial_\tau v_1=-\mathrm{i}\xi v_1+\frac{1}{2}ev_2, \tag{15}$$

$$\partial_\tau v_2=\mathrm{i}\xi v_1+\frac{1}{2}e^*v_1, \tag{16}$$

$$\partial_x e=2(v_1v_2^*), \tag{17}$$

where $e=\varphi\exp(-2\mathrm{i}\xi\tau)$ is the new photonic field, $\tau=t-x$ is the new time, $y=\frac{\rho}{2}x$ is the scaled coordinate and ξ is the parameter accounting for the detuning of the photon field from the resonance of the two-level system.

The equations (15), (16) are Zakharov–Shabat equations [39] and the system (15)–(17) has a soliton solution [40]

$$v_1=-\mathrm{sech}(2\beta\eta)\cos(\theta)\exp(\mathrm{i}\xi\eta), \tag{18}$$

$$v_2=\sinh(2\beta\tau+\mathrm{i}\theta)\mathrm{sech}(2\beta\eta)\exp(\mathrm{i}\xi\eta), \tag{19}$$

$$e=4\beta\,\mathrm{sech}(2\beta\eta)), \tag{20}$$

where β is the amplitude of the soliton, $\theta=-a\tan(\xi/\beta)$ and $\eta=\tau-\frac{\cos^2\theta}{4\beta^2}y$. In SIT solitons the optical field excites the TLS but then return it exactly to the ground state. So SIT solitons are very different from the optical soliton appearing because of nonlinear modification of the refractive index of the propagation medium (solitons in nonlinear Schrödinger equation, NLS solitons). The fact that the optical field must return the two-level

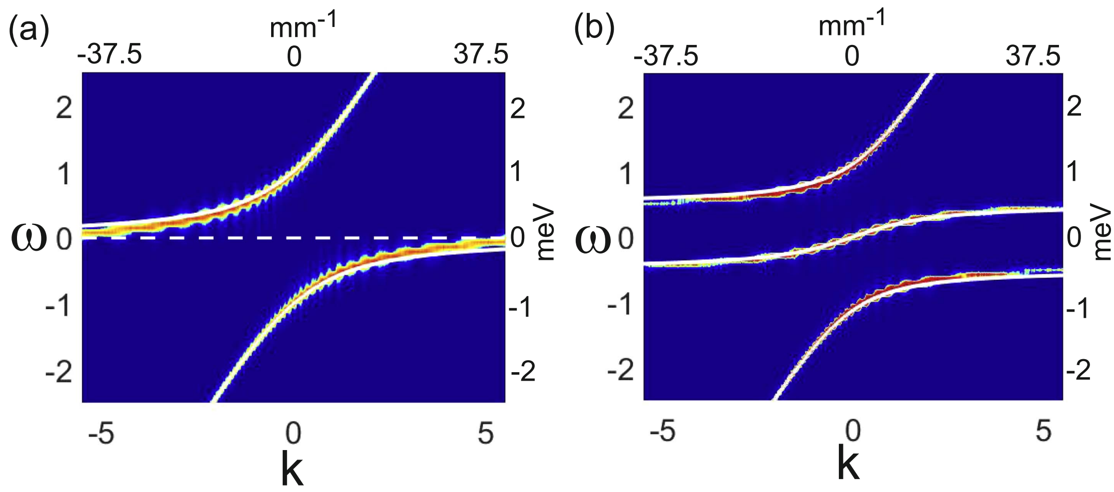

Figure 2. Spatial-temporal spectral representation of the field φ. The plotted quantity is $|\int \varphi^{(R)}(t', x')\mathrm{e}^{\mathrm{i}\omega t' - \mathrm{i}kx'}\mathrm{d}x'\mathrm{d}t'|^2$ averaged over 30 simulations. The white lines show the analytical dependencies of the frequency of the linear excitations on their wavenumber derived in the continuous limit. The dashed line corresponds to the mode without photonic component, the dispersions of the other modes are shown by solid lines. The atoms are in the ground state $S_z^R = S_z^L = -\frac{1}{2}$, the number of atoms is 399, the length of the system is 200 which means that the atom density is $\rho = 2$. Panel (a) corresponds to zero magnetic field $\Omega = 0$ and panel (b) to the magnetic field $\Omega = 1$. The dimensionless unit of frequency corresponds to 1 meV in physical units, the wavevector 7.6 mm^{-1} corresponds to 1 in dimensionless units.

medium back to the ground state imposes a condition (known as area theorem) on the are of the optical field and thus SIT solitons are often referenced as 2π solitons.

3. Effect of the transverse magnetic field on the spectrum of linear excitations

In the present paper we focus on the effect of the magnetic field Ω on the dynamics of the pulses in the two levels media. All the approximations made, we then analyze the resulting equations. We first start from the linear limit: in this case we assume that all the atoms are in their ground state $S_z^{(R,L)} = -1/2$. We then write down the dispersion equation in the linear case:

$$2\left(\omega^2 - \frac{\Omega^2}{4}\right)(\omega - k) = \rho\omega. \tag{21}$$

The dispersion relation is shown in figure 2. This dispersion is similar to the dispersion appearing because of electromagnetically induced transparency [43, 44] and also allows to obtain slow light. It is seen that the dispersion splits into three branches, and the central branch is characterized by low group velocity vanishing at $\Omega = 0$. Thus the excitations belonging to this branch can be referred as slow light. The background is the spectral representation of the evolution of the photonic field obtained from direct numerical simulations. The initial conditions for the numerical simulation was a low intensity noise and to make the background smooth we did averaging over 30 simulations.

In the absence of the magnetic field $\Omega = 0$ the intermediate branch shown by the dashed white line in panel (a) corresponds to the oscillations of $S_-^{(L)} - S_z^{(L)}$ subsystem which is decoupled from both the photonic field and from the $S_-^{(R)} - S_z^{(R)}$ subsystem. This explains why this branch of the dispersion characteristic is absolutely flat and not visible in the spectral background obtained from the direct numerical simulations.

In the same time both the upper and the lower branches match well to the intense spectral patterns of the background. The splitting between the upper and the lower dispersion branches is controlled by the density of the atoms ρ (and in physical units, of course, by the coupling strength between the atoms and the photons). The hybridization is significant only in the vicinity of the resonance and so at large detuning from the resonance one of the dispersion characteristics becomes close to the dispersion of free photons and the other dispersion branch becomes a horizontal line corresponding to free oscillations of the spin of the atoms (the atoms do not interact directly but through the photons).

Panel (b) illustrate the case with magnetic field $\Omega = 1$. It is seen that because of the coupling to the opposite spins and through it to the photonic subsystem the intermediate branch forms a finite though a narrow band . The coupling to the photons makes the line visible on the spectrum calculated for the photonic component. The

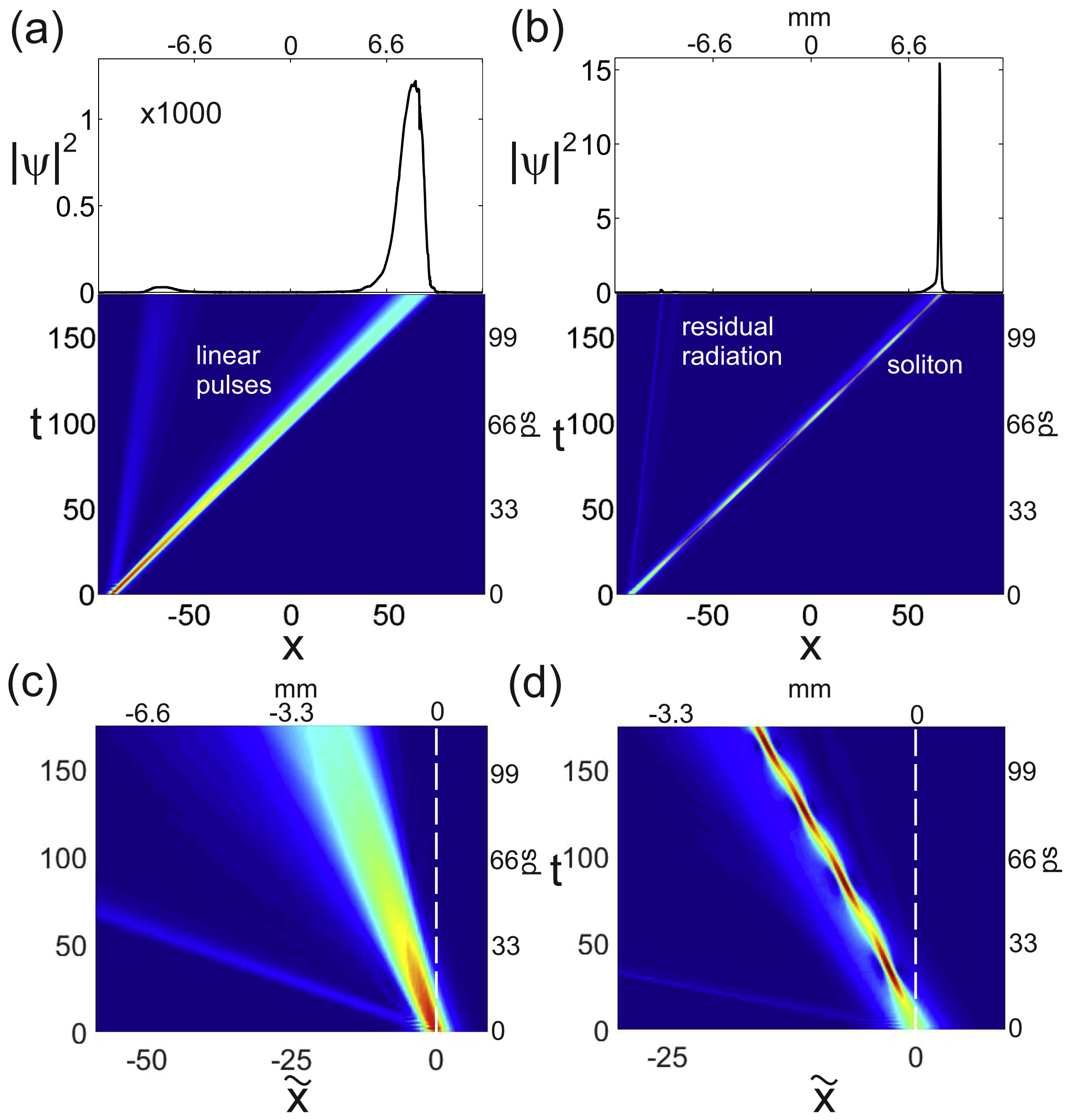

Figure 3. The evolution of the photonic component φ of the pulse in the linear (a) and in the soliton regimes (b). Panels (c) and (d) show the linear and nonlinear evolutions of the pulses in the reference frame $t\tilde{x} = x - vy - x_{0\varphi}$) moving with the velocity equal to the velocity of light in the fiber. The vertical dashed lines show where the centers of the pulses would be situated if the pulses propagated with the velocity equal to the velocity of light in the fiber. The initial condition is taken in the form $\varphi(x,\ t = 0) = a_\varphi\ \mathrm{sech}((x - x_{0\varphi})/w_{0\varphi})\exp(\mathrm{i}k_\varphi x)$. For the linear case $a_\varphi = 0.02$ and for the nonlinear $a_\varphi = 2$. The other parameters are $\Omega = 0, k_\varphi = 2.5, w_{0\varphi} = 1.5, x_{0\varphi} = -92, S_-^R = S_-^L = 0$, $S_z^R = S_z^L = -\frac{1}{2}$. The dimensionless unit length corresponds to 132 μm in physical units, the dimensionless unit of time—0.66 ps.

group velocity of the modes belonging to the intermediate branch can be efficiently controlled by the magnetic field and the regime of slow light can be achieved easily.

Now let us consider propagation of optical pulses in the systems in question. We start from the case of zero magnetic field $\Omega = 0$. In our numerical simulations we take the initial conditions in the form $\varphi(x,\ t = 0) = a_\varphi\ \mathrm{sech}((x - x_{0\varphi})/w_{0\varphi})\exp(\mathrm{i}k_\varphi x)$, where a_φ is the amplitude, k_φ is the wavevector, $w_{0\varphi}$ is the width and $x_{0\varphi}$ is the initial position of the pulse. All atoms are initially in the ground states $S_-^R = S_-^L = 0,\ S_z^R = S_z^L = -\frac{1}{2}$.

The regime of the linear propagation is shown in panel (a) of figure 3. It is seen that the pulse splits in two components and most of the energy goes to the quasi-photonic mode. It is also seen that because of the interaction with two-level medium the pulses propagate slower than the light in the fiber. The pulse spreads significantly with the propagation and the dispersion makes the shape of the pulse to be asymmetric.

3.1. Nonlinear propagation of optical pulses

The dynamics of the intense pulses is very different. As one can see in panel (b) of figure 3 the spreading of the intense pulse is suppressed and a solitary wave forms. The physical origin of the localization is that the front part

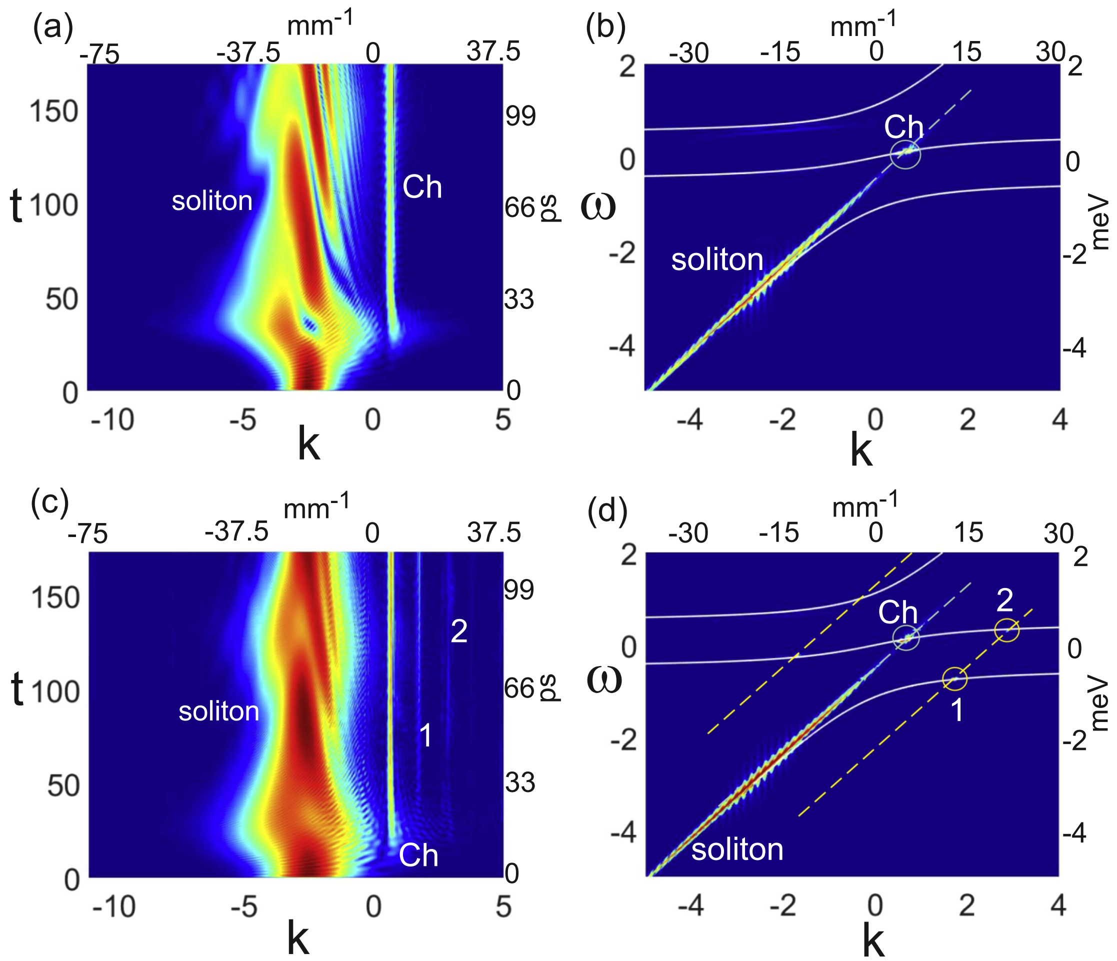

Figure 4. The evolution of the spatial spectrum (a) and the spatio-temporal spectrum of the photonic component (b) are shown for the case of magnetic field $\Omega = 1$. The initial conditions are the same as in figure 3. The resonant Cherenkov radiation is marked as 'Ch'. Panels (c) and (d) illustrate the propagation in the presence of the spatially varying magnetic field $\Omega = \Omega_0 + \Delta\sin(\kappa x), \Omega_0 = 1$, $\Delta = 0.3$ and $\kappa = 2$. The additional observed resonances are marked as '1' and '2.' To make the resonant radiation spectral lines more visible the initial pulse is taken with larger amplitude $a_\varphi = 2.5$ and smaller width $w_{0\varphi} = 0.8$. The dimensionless unit of time corresponds to 0.66 ps in physical units, the wavevector 7.6 mm^{-1} corresponds to 1 in dimensionless units, the dimensionless frequency unit is equivalent to 1 meV.

if the photonic pulse excites the spins but then rear part of the pulse absorbs the photonic excitation. There is the intensity of the pulse when the rear part of the photonic pulse removes energy from the spin subsystem completely. So the propagation of the pulse does not perturb the atom subsystem and the dispersion of the pulse caused by the coupling of the atoms and the photons is suppressed. As it is discussed above this process is very much similar to the formation of SIT solitons in TLSs. It should be mentioned here that weak dispersive waves seen in figure 3 are the residual radiation that is left of the initial pulse after the formation of the soliton. Since the initial distribution is not an exact soliton we see slow oscillations of the soliton and its overlap with the residual radiation, panel (d) of figure 3. Let us note that the oscillations of the solitons can be important for example from the point of view of radiation effects but they are out of the scope of the present paper and will be considered elsewhere.

Now let us study the influence of the magnetic field on the propagation of the solitary waves in the considered systems. The interesting phenomenon observed in the presence of the magnetic field is that a weak but clearly visible radiation tail grows behind the solitary wave. In the spatial spectrum of the field a narrow line appears indicating that the radiation is resonant, see figure 4. Let us mention that the evolution of the soliton spectrum takes place because the initial pulse is not an exact soliton solution and the localized modes get excited.

The observed radiation can be interpreted as Cherenkov radiation of an optical solitary wave coupled to atomic system. In the optical context this effect was reported for the first time back in 1986 [45], the theory of the radiation then was developed in [46]. Similar effects were also found in different physical systems, for example in superconducting systems [47–49] and in the arrays of optical micro-resonators [50].

The radiation occurs when a spatial harmonic of the soliton has a velocity equal to phase velocity of the linear eigenmode of the system. Since a solitary wave moves as a whole without changes of the shape, all spatial harmonics of the soliton move with the velocity of the soliton. So the frequencies ω of the spatial harmonics of the soliton are expressed through their wave vectors k as $\omega = \omega_s + v_s(k - k_s)$ where ω_s is the central frequency of the soliton, v_s is the soliton velocity and k_s id the wavevector of the soliton. From this one can easily derive the condition of the resonant emission of the dispersive wave by a solitary wave

$$\omega(k_r) = \omega_s + v_s(k_r - k_s), \tag{22}$$

where k_r is the wavevector of the resonant dispersive wave.

As it is mentioned above all spatial harmonics of the soliton move with the same velocity and thus in $\omega - k$ representation the spectral pattern of the soliton is a stripe along the line $\omega = \omega_s + V_s(k - k_s)$. Most of the soliton energy is in the harmonics with $k \approx k_s$ and that is why the soliton spectral pattern has maximum of intensity at k_s, which is clearly seen in the soliton spectral pattern shown figure 4(b).

The resonance condition (22) is satisfied if the soliton spectral pattern crosses the dispersion characteristic of the linear excitations. As it is seen in panel (b) the crossing with the intermediate branch takes place and at this crossing a narrow bright spot is seen. The position of this bright spot exactly coincide with the narrow spectral line seen in panel (a). So we can interpret the appearance of new spectral line as resonant excitation of slow light by propagating solitary wave. Let us remark that without the magnetic field the modes belonging to the intermediate branch do not interact with the solitary wave and so the radiation is absent. It is also worth mentioning that the soliton spectral pattern can cross neither the low no upper branch of the dispersion characteristic, so the resonant emission in these modes is impossible.

For sake of completeness we consider the case when the soliton propagate in a spatially periodic system. As an example we study the case when the magnetic field is a periodic function of the coordinate x. Then the propagation of the soliton produces several resonant lines in the spectrum, see panel (c) of figure 4. This can be understood as an analog of transitional radiation of soliton or Cherenkov radiation of Bloch waves [51]. To describe the additional resonances the resonant condition (22) has to be modified as follows

$$\omega(k_r) = \omega_s + v_s(k_r - k_s + \kappa \cdot m), \tag{23}$$

where $\kappa = \frac{2\pi}{L}$, L is the spatial period of the magnetic field modulation and m is an integer. The resonance condition (23) accounts for the fact that the spatial harmonics of the soliton mixes with mth harmonics of the magnetic field modulation and this component can be in the resonance with a linear wave.

Graphical solution of the resonant condition (23) is shown in panel (d) for $m = [-1, 0, 1]$. Apart from the Cherenkov synchronism another four resonances are seen. The resonances marked as '1' and '2' are visible in the spectra well. The frequencies of the other two resonances overlaps with the soliton spectrum and so cannot be resolved in panel (c). However at close look at the spectrum shown in panel (d) the spectral maxima corresponding to these resonances are visible exactly where they are predicted by the resonance condition. It is interesting to note that in the presence of periodic modulation the waves belonging to the upper and the lower dispersion branches can be resonantly excited by the propagating solitary wave.

It is shown that in the presence of the magnetic field intense pulses can resonantly excite slow light. This effect can potentially be used for writing and storing information in slow light pulses. Now we consider how this information can be read. It can be done by the transformation of the slow light back into the propagating photonic modes. Here we consider how resonant scattering of the slow light on optical solitary waves produces new fast propagating pulses of low intensity.

3.2. Scattering of dispersive waves on SIT solitons

In order to study the scattering of linear waves on the solitons in the presence of the magnetic field we take the initial condition in the form of the intense pulse having only the photonic component and a pulse of low intensity having only atomic component. The excited atomic component splits into two pulses belonging either to the intermediate and the lower or to the intermediate and the upper branches of the dispersion characteristics and thus having different frequencies. The excited photonic component produces a solitary wave and weak residual radiation.

The formation and the propagation of the pulses are illustrated in panel (a) of figure 5. It is seen that the intense pulse propagates without any visible spreading but the radiation appears behind the soliton. As it is discussed above this is a resonant radiation of the soliton. The corresponding spectral line appears in the spectrum of the photonic field, see panel (b). At a certain moment the soliton collide with the slow pulses formed from the seeded excitation of the atomic system. Approximately at the same time two new narrow lines marked as '1' and '2' appear in the spectrum. These lines as well as the Cherenkov line are clearly visible in the spatial spectrum calculated at $t = 180$, see panel (c).

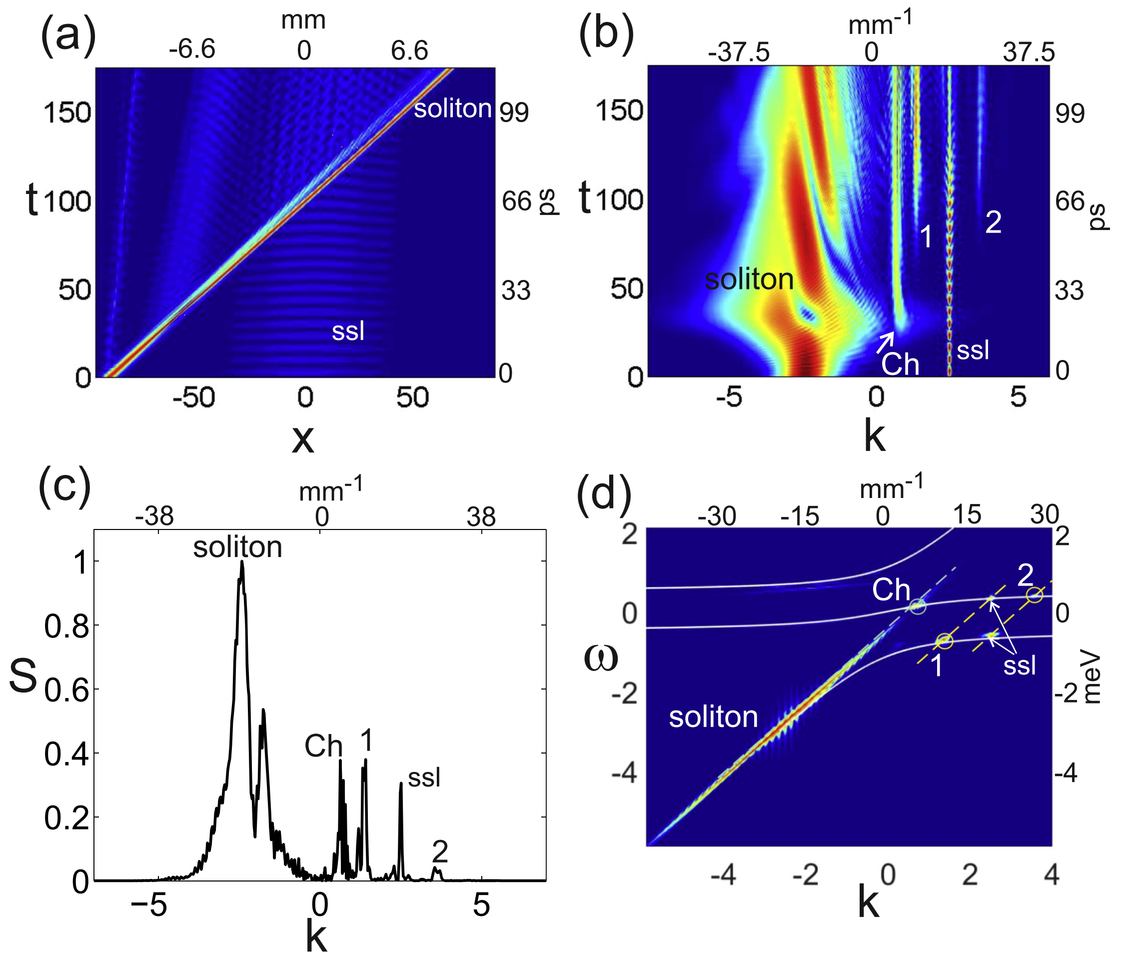

Figure 5. The evolution of the photonic component φ (a), the evolution of the spatial spectrum (b), the spatial spectrum at $t = 180$ and spatial-temporal spectrum illustrating joint propagation of intense and weak dispersive pulses. The spectral signatures of the seeded slow light pulses are marked as 'ssl'. The initial condition is taken in the form $\varphi(x,\ t=0) = a_\varphi\ \mathrm{sech}((x - x_{0\varphi})/w_{0\varphi})\exp(ik_\varphi x)$ and S_y^R with $a_\varphi = 2.,k_\varphi = 2.5, w_{0\varphi} = 1.5, x_{0\varphi} = -92$. The initial state of the atom subsystem is $S_-^R = 0,\ S_z^R = -\frac{1}{2},\ S_{z\,j}^L = -\frac{1}{2} + a_A\exp(-\left(\frac{d_0 j}{w_A}\right)^2)$, $S_{-\,j}^L = \sqrt{\frac{1}{4} - S_{z\,j}^{(R)\,2}}\ \exp(ik_A d_0 j)$, where $a_A = 0.075$ is the amplitude of the initial excitation, $w_A = 25$ is its width, $k_A = 2.5$ is the excitation wavevector and $d_0 = 0.5$ is the distance between the atoms. The magnetic field is $\Omega = 1$. The dimensionless unit of time corresponds to 0.66 ps in physical units, the dimensionless unit of length corresponds to 132 μm, the wavevector 7.6 mm^{-1} corresponds to 1 in dimensionless units, the dimensionless unit of frequency corresponds to 1 meV.

To understand the origin of the spectral lines marked as '1' and '2' it is necessary to consider a three wave mixing process between the solitons and the dispersive waves [52]. A similar four wave mixing process is well known in nonlinear optics and was studied both theoretically [53] and experimentally [54, 55]. It has been shown that this process can be very efficient from the point of view new frequency generation and that it plays an important role in optical supercontinuum generation [56–58].

Here we sketch the derivation of the resonant scattering. The nonlinearity results in the mixing of the spatial harmonics of the soliton with the seeded dispersive wave. Thus in the reference frame moving with the soliton the driving force is a spatially localized function oscillating at the frequency equal to the detuning of the soliton frequency from the frequency of the dispersive wave. After simple algebra one can show that the driving force is in the resonance with an eigenmode of the medium if the following resonance condition is satisfied

$$\omega(k_r) = \omega_s \pm (\omega(k_{\mathrm{dw}}) + v_s(k_r - k_{\mathrm{dw}}) - \omega_s), \tag{24}$$

where k_{dw} is the wavevector of the seeded dispersive wave.

Now let us discuss spectrum shown in panel (d) of figure 5. The atomic excitations with the wavevector k_A produces two envelopes of slow light with $k_{\mathrm{dw}} \approx k_A$. However these pulses belong to different branches of the dispersion characteristic (in this example to the upper and the intermediate ones) and have different frequencies ω_{dw}. The spectral features corresponding to these envelopes are marked as 'ssl' (seeded slow light).

The graphic solution of (24) for sign + is shown in panel (d) over the spatial-temporal spectrum of the field for two pulses formed from the seeded pulse. The crossing of the dashed orange line with the dispersion characteristic of the linear waves indicates the resonance. One can see that the resonance condition predicts the positions of the

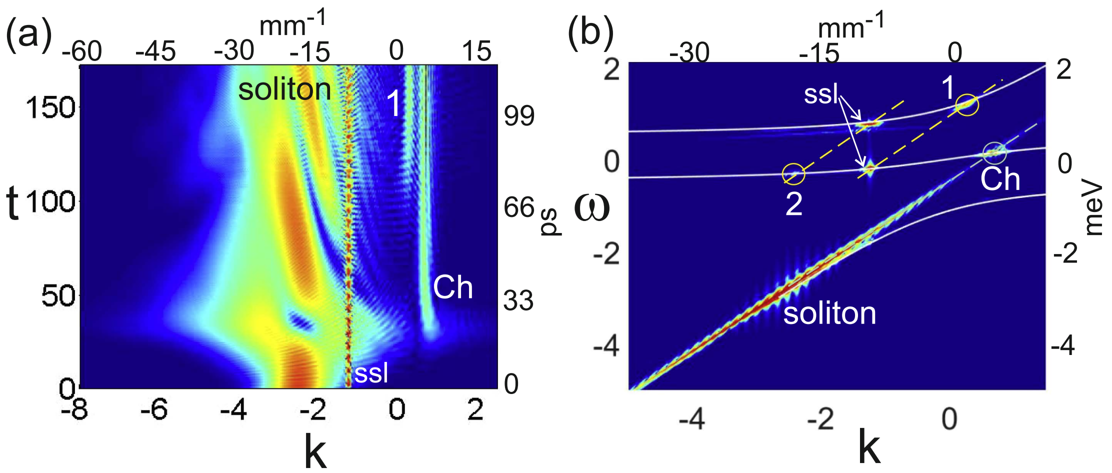

Figure 6. The evolution of the spatial spectrum (a) and spatial-temporal spectrum (b) illustrating joint propagation of intense and weak dispersive pulses. The parameters and the initial conditions are the same as for figure 5 but the wavevector of the atomic subsystem excitation has the opposite sign $k_A = -2.5$. The dimensionless unit of time corresponds to 0.66 ps in physical units, the wavevector 7.6 mm^{-1} corresponds to 1 in dimensionless units, the dimensionless frequency corresponds to 1 meV.

resonances '1' and '2' very well. It is worth mentioning here that the sign—in (24) give a second resonance but the coupling of the driving force with this resonant mode is weak and so the resonant radiation is not seen.

In the example considered above the soliton nestles on the lower mode and the scattering goes either from the intermediate mode to the lower one or vice versa. Changing the parameters of the seeded slow light excitation it is possible to obtain the scattering between the intermediate and the upper modes.

Figure 6 illustrate the case when the seeded pulse splits into two envelopes belonging to the intermediate and the upper mode. When the dispersive waves of the intermediate branch collide with the soliton the waves belonging to the upper branch get excited. In its turn when the envelope of the dispersive waves belonging to the upper branch collide with the soliton the scattering goes into the modes of the intermediate branch of the dispersion characteristics.

So it is shown that solitary waves propagating in the considered system allows to generate new optical frequencies and to provide inter modes switching of the dispersive waves.

4. Conclusions

We have studied the nonlinear dynamics of a chiral system comprising a one-dimensional array of TLSs in the transverse magnetic field coupled via common chiral photonic reservoir. We have shown, that the transverse magnetic field results in the emergence of the slow light branch in the photonic spectrum. Finally, the processes of the stimulated excitation of slow light by solitons as well as excitation of dispersive waves via the scattering of soliton on slow light mode have been modeled. This process constitutes the basis for the perspective realizations of optical memory based on the chiral photonic systems.

We would also like to mention that the accounting for the fiber dispersion results in the additional terms in equation (5) and this affects propagation of the optical pulses. However, first, the fiber dispersion can be made very small and so the results for dispersionless fibers are of physical importance. Secondly, the dispersion and Kerr nonlinearity do not necessarily destroy SIT solitons but can result in the formation of mixed SIT-NLS solitons, [40–42]. Of course SIT-NLS solitons require a separate consideration but one can anticipate that the resonant interaction between the solitons and the dispersive waves would remain qualitatively the same as for pure SIT solitons.

Acknowledgments

The authors thank Dr MI Petrov for enlightening discussions. The work was by megagrant 14.Y26.31.0015 and Goszadanie no 3.261 4.2017/4.6 and 3.1365.2017/4.6 of the Ministry of Education and Science of Russian Federation. IVI and IAS acknowledges support from the Icelandic Research Fund, Grant No. 163082-051. IVI thanks Grant of President of Russian Federation MK-6248.2018.2, RFBR project 16-32-60123, and University of Iceland for hospitality. The work of AVY was financially supported by the Government of the Russian Federation (Grant 074-U01) through ITMO Fellowship scheme.

References

[1] Chang A M 2003 Chiral Luttinger liquids at the fractional quantum Hall edge *Rev. Mod. Phys.* **75** 1449–505
[2] Bansil A, Lin H and Das T 2016 Topological band theory *Rev. Mod. Phys.* **88** 021004
[3] Hasan M Z and Kane C L 2010 Topological insulators *Rev. Mod. Phys.* **82** 3045
[4] Haldane F D M and Raghu S 2008 Possible realization of directional optical waveguides in photonic crystals with broken time-reversal symmetry *Phys. Rev. Lett.* **100** 013904
[5] Wang Z, Chong Y D, Joannopoulos J D and Soljačić M 2008 Reflection-free one-way edge modes in a gyromagnetic photonic crystal *Phys. Rev. Lett.* **100** 013905
[6] Wang Z, Chong Y, Joannopoulos J D and Soljačić M 2009 Observation of unidirectional backscattering-immune topological electromagnetic states *Nature* **461** 772–5
[7] Hafezi M, Demler E A, Lukin M D and Taylor J M 2011 Robust optical delay lines with topological protection *Nat. Phys.* **7** 907–12
[8] Fang K, Yu Z and Fan S 2012 Realizing effective magnetic field for photons by controlling the phase of dynamic modulation *Nat. Photon.* **6** 782–7
[9] Rechtsman M C, Zeuner J M, Plotnik Y, Lumer Y, Podolsky D, Dreisow F, Nolte S, Segev M and Szameit A 2013 Photonic Floquet topological insulators *Nature* **496** 196–200
[10] Khanikaev A B, Hossein Mousavi S, Tse W-K, Kargarian M, MacDonald A H and Shvets G 2013 Photonic topological insulators *Nat. Mater.* **12** 233–9
[11] Lu L, Joannopoulos J D and Soljačić M 2014 Topological photonics *Nat. Photon.* **8** 821–9
[12] Kavokin A V, Baumberg J J, Malpuech G and Laussy F P 2011 *Microcavities* (Oxford: Oxford University Press)
[13] Carusotto I and Ciuti C 2013 Quantum fluids of light *Rev. Mod. Phys.* **85** 299–366
[14] Schneider C *et al* 2013 An electrically pumped polariton laser *Nature* **497** 348–52
[15] Nalitov A V, Solnyshkov D D and Malpuech G 2015 Polariton Z topological insulator *Phys. Rev. Lett.* **114** 116401
[16] Gulevich D R, Yudin D, Iorsh I V and Shelykh I A 2016 Kagome lattice from an exciton-polariton perspective *Phys. Rev.* B **94** 115437
[17] Gulevich D R, Yudin D, Skryabin D V, Iorsh I V and Shelykh I A 2017 Exploring nonlinear topological states of matter with exciton-polaritons: edge solitons in kagome lattice *Sci. Rep.* **7** 1780
[18] Bliokh K Y, Rodriguez-Fortuno F J, Nori F and Zayats A V 2015 Spin–orbit interactions of light *Nat. Photon.* **9** 796–808
[19] Bliokh K Y, Smirnova D and Nori F 2015 Quantum spin Hall effect of light *Science* **348** 1448–51
[20] Bliokh K Y and Nori F 2012 Transverse spin of a surface polariton *Phys. Rev.* A **85** 061801(R)
[21] Rodriguez-Fortuño F J, Marino G, Ginzburg P, O'Connor D, Martinez A, Wurtz G A and Zayats A V 2013 Near-field interference for the unidirectional excitation of electromagnetic guided modes *Science* **340** 328–30
[22] Van Mechelen V and Jacob Z 2016 Universal spin-momentum locking of evanescent waves *Optica* **3** 118–26
[23] Rodriguez-Fortuño F J, Engheta N, Martinez A and Zayats A V 2015 Lateral forces on circularly polarizable particles near a surface *Nat. Commun.* **6** 8799
[24] Hayat A, Balthasar Mueller J P and Federico C 2015 Lateral chirality-sorting optical forces *Proc. Natl Acad. Soc.* **112** 13190–4
[25] Petrov M I, Sukhov S V, Bogdanov A A, Shalin A S and Dogariu A 2016 Surface plasmon polariton assisted optical pulling force *Laser Photonics Rev.* **10** 116–22
[26] Yuen-Zhou J, Saikin S K, Zhu T, Onbasli M C, Ross C A, Bulovic V and Baldo M A 2016 Plexciton Dirac points and topological modes *Nat. Commun.* **7** 11783
[27] Kapitanova P V, Ginzburg P, Rodriguez-Fortuño F J, Filonov D S, Voroshilov P M, Belov P A, Poddubny A N, Kivshar Y S, Wurtz G A and Zayats A V 2014 Photonic spin Hall effect in hyperbolic metamaterials for polarization-controlled routing of subwavelength modes *Nat. Commun.* **5** 3226
[28] Coles R J, Price D M, Dixon J E, Royall B, Clarke E, Kok P, Skolnick M S, Fox A M and Makhonin M N 2016 Chirality of nanophotonic waveguide with embedded quantum emitter for unidirectional spin transfer *Nat. Commun.* **7** 1183
[29] Pichler H, Ramos T, Daley A J and Zoller P 2015 Quantum optics of chiral spin networks *Phys. Rev.* A **91** 042116
[30] Ramos T, Vermersch B, Hauke P, Pichler H and Zoller P 2016 Non-Markovian dynamics in chiral quantum networks with spins and photons *Phys. Rev.* A **93** 062104
[31] Chang D E, Vuletic V and Lukin M D 2014 Quantum nonlinear opticsphoton by photon *Nat. Photon.* **8** 685
[32] Corzo N V, Gouraud B, Chandra A, Goban A, Sheremet A S, Kupriyanov D V, Laurat J and Large B 2016 Reflection from one-dimensional chains of trapped atoms near a nanoscale waveguide *Phys. Rev. Lett.* **117** 133603
[33] Sørensen H L, Béguin J-B, Kluge K W, Iakoupov I, Sørensen A S, Müller J H, Polzik E S and Appel J 2016 Coherent backscattering of light off one-dimensional atomic strings *Phys. Rev. Lett.* **117** 133604
[34] Pletyukhov M and Gritsev V 2012 Scattering of massless particles in one-dimensional chiral channel *New J. Phys.* **14** 095028
[35] Kornovan D F, Petrov M I and Iorsh I V 2017 Transport and collective radiance in a basic quantum chiral optical model *Phys. Rev.* B **96** 115162
[36] MaCall S L and Hahn E L 1967 Self-induced transparency by pulsed coherent light *Phys. Rev. Lett.* **18** 908
[37] MaCall S L and Hahn E L 1969 Self-induced transparency *Phys. Rev.* **183** 457
[38] Lamb G L Jr 1971 Analytical descriptions of ultrashort optical pulse propagation in a resonant medium *Rev. Mod. Phys.* **43** 99
[39] Zakharov V E and Shabat A B 1971 Exact theory of two-dimensional self-focusing and one-dimensional self-modulation of wave in nonlinear media *Zh. Eksp. Teor. Fiz.* **61** 118
Zakharov V E and Shabat A B 1972 *Sov. Phys.—JETP* **34** 62
[40] Masataka N, Eiichi Y and Hirokazu K 1991 Coexistence of a self-induced-transparency soliton and a nonlinear Schrödinger soliton in an erbium-doped fiber *Phys. Rev.* A **44** 5973
[41] Maimistov A I and Manykin E A 1983 Propagation of ultrashort optical pulses in resonant nonlinear light guides *Zh. Eksp. Teor. Fiz.* **85** 1177
Maimistov A I and Manykin E A 1983 *Sov. Phys.—JETP* **58** 685
[42] Mel'nikov I V, Nabiev R F and Nazarkin A V 1990 Coherent amplification of ultrashort solitons in doped fibers *Opt. Lett.* **15** 1348
[43] Hau L V, Harris S E, Dutton Z and Behroozi C H 1999 Light speed reduction to 17 metres per second in an ultracold atomic gas *Nature* **397** 594–8
[44] Fleischhauer M, Imamoglu A and Marangos J P 2005 Electromagnetically induced transparency: optics in coherent media *Rev. Mod. Phys.* **77** 633–73
[45] Wai P K A, Menyuk C R, Lee Y C and Chen H H 1986 Nonlinear pulse propagation in the neighborhood of the zero-dispersion wavelength of monomode optical fibers *Opt. Lett.* **11** 464–6

[46] Akhmediev N and Karlsson M 1995 Cherenkov radiation emitted by solitons in optical fibers *Phys. Rev.* A **51** 2602–7
[47] Kurin V V and Yulin A V 1997 Radiation of linear waves by solitons in a Josephson transmission line with dispersion *Phys. Rev.* B **55** 11659–69
[48] Kurin V V, Yulin A V, Shereshevskii I A and Vdovicheva N K 1998 Cherenkov radiation of vortices in a two-dimensional annular Josephson junction *Phys. Rev. Lett.* **80** 3372–5
[49] Wallraff A, Ustinov A V, Kurin V V, Shereshevsky I A and Vdovicheva N K 2000 Whispering vortices *Phys. Rev. Lett.* **84** 151–4
[50] Savelev R S, Yulin A V, Krasnok A E and Kivshar Y S 2016 Solitary waves in chains of high-index dielectric nanoparticles *ASC Photonics* **3** 1869–76
[51] Yulin A V, Skryabin D V and Russell P St J 2003 Transition radiation by matter-wave solitons in optical lattices *Phys. Rev. Lett.* **91** 260402
[52] Yulin A V, Skryabin D V and Russell P St J 2004 Four-wave mixing of linear waves and solitons in fibers with higher-order dispersion *Opt. Lett.* **29** 2411–3
[53] Skryabin D V and Yulin A V 2005 Theory of generation of new frequencies by mixing of solitons and dispersive waves in optical fibers *Phys. Rev.* E **72** 016619
[54] Efimov A, Yulin A V, Skryabin D V, Knight J C, Joly N, Omenetto F G, Taylor A J and Russell P 2005 Interaction of an optical soliton with a dispersive wave *Phys. Rev. Lett.* **95** 213902
[55] Efimov A, Taylor A J, Yulin A V, Skryabin D V and Knight J C 2006 Phase-sensitive scattering of a continuous wave on a soliton *Opt. Lett.* **31** 1624–6
[56] Skryabin D V and Gorbach A V 2010 Looking at a soliton through the prism of optical supercontinuum *Rev. Mod. Phys.* **82** 1287–99
[57] Yulin A V, Driben R, Malomed B A and Skryabin D V 2013 Soliton interaction mediated by cascaded four wave mixing with dispersive waves *Opt. Express* **21** 14481–6
[58] Driben R, Yulin A V, Efimov A and Malomed B A 2013 Trapping of light in solitonic cavities and its role in the supercontinuum generation *Opt. Express* **21** 19091–6